Scripta Materialia 122 (2016) 72–76

Contents lists available at ScienceDirect

Scripta Materialia

journal homepage: www.elsevier.com/locate/scriptamat

Regular Article

Porosity regrowth during heat treatment of hot isostatically pressed additively manufactured titanium components

S. Tammas-Williams [a,*], P.J. Withers [b], I. Todd [a], P.B. Prangnell [b]

[a] Department of Materials Science and Engineering, University of Sheffield, Sheffield S1 3JD, UK
[b] School of Materials, University of Manchester, Manchester M13 9PL, UK

ARTICLE INFO

Article history:
Received 16 March 2016
Received in revised form 28 April 2016
Accepted 1 May 2016
Available online 24 May 2016

Keywords:
Additive manufacture
Selective electron beam melting (SEBM)
Pores
Heat treatment
Hot isostatic pressing (HIPing)

ABSTRACT

X-ray computed tomography has been used to track the behaviour of individual pores found in selective electron beam melted additive manufactured titanium. Porosity was found to shrink below the detection limit of X-ray microtomography (<5 μm) upon hot isostatic pressing. Spherical argon containing gas pores, which have a high internal gas pressure following hot isostatic pressing, have been found to progressively reappear and grow in proportion to their original as-built size during high temperature (β-anneal) treatments, whereas larger irregular low pressure pores did not reappear. The implications of these observations in terms of additive manufacturing are discussed.

In additive manufacturing (AM), complex components can be produced directly from CAD models by the sequential deposition and consolidation of 2D layers of material [1,2]. The benefits of this new manufacturing approach have been well documented in the literature [1,2]. However, with powder bed AM, residual gas porosity and lack of fusion defects (LOFDs) are known issues [3] that, if not adequately controlled, can cause a significant knockdown in fatigue life of components [4]. In powder bed AM, irregular LOFDs arise when the melt pool is too small to fully fuse the powder, while gas pores originate from bubbles which are trapped in the melt pool on solidification and have a near spherical morphology [5]. In the powder bed AM process selective electron beam melting (SEBM) of titanium, gas pores have been shown to dominate the number fraction of the total porosity present (>95%) [5]. Although their overall volume fraction is low (<0.2% [5]), the high frequency of such gas pores means that SEBM fatigue samples often fail from cracks initiating at this type of defect [4]. To solve this problem, many aerospace companies are considering applying post-build hot isostatic pressing (HIPing) treatments to AM components. It has been reported that HIPIng of AM parts is very effective at closing porosity, which reduces internal stress concentrations, with a consequent increase in fatigue life [2,6].

Recently, the current authors used high resolution 3D X-ray computed tomography (CT) to confirm that, with SEBM, all the as-built internal pores could be removed/shrunk by a standard HIP cycle (Fig. 1b) to below the detection limit of the equipment used (~5 μm) [6]. Here, we aim to examine the effect of applying a typical β-anneal heat treatment on the porosity closed by HIPing. Since SEBM is carried out in a vacuum chamber, at a pressure <1 Pa, the gas pores found in built components mainly originate from bubbles of argon that were originally trapped in the feedstock powder particles during atomisation, some of which are subsequently unable to escape from the melt pool during SEBM. Argon has an atomic radius too large for significant solubility in titanium [7] and thus, following HIPing, some argon containing pores might be expected to survive in the material, but at a significantly smaller size and higher internal pressure. Indeed, if equilibrium is reached the pore pressure could equal the HIPing pressure of around 100 MPa.

To examine whether a typical β-annealing treatment would result in pore growth in HIPed AM components, CT scanning was performed on the same sample after manufacture by SEBM, after HIPing under a 100 MPa pressure at 920 °C for 2 h (see ref. [6]), and following annealing for different times and temperatures, so that individual pores could be tracked at each stage within the sample. The sample comprised a 10 mm high, 1.7 mm diameter, cylinder having an axis aligned with the build direction, machined from the centre edge of the face of a $10 \times 10 \times 15\ mm^3$ cuboid sample. The cuboid sample was manufactured with argon gas atomised, Ti–6Al–4V powder in an Arcam AB SEBM system using standard operating conditions (see refs. [5,6,8] for details). This consisted of first melting the perimeter of each 2D layer by 'contouring', before consolidating the internal area using a snaking 'hatching' pattern. The cylinder was deliberately machined from the contour-hatch overlap region, which prior work has shown contains a relatively high number density of LOFDs and gas pores [5].

* Corresponding author.
E-mail address: s.tammas-williams@sheffield.ac.uk (S. Tammas-Williams).

http://dx.doi.org/10.1016/j.scriptamat.2016.05.002

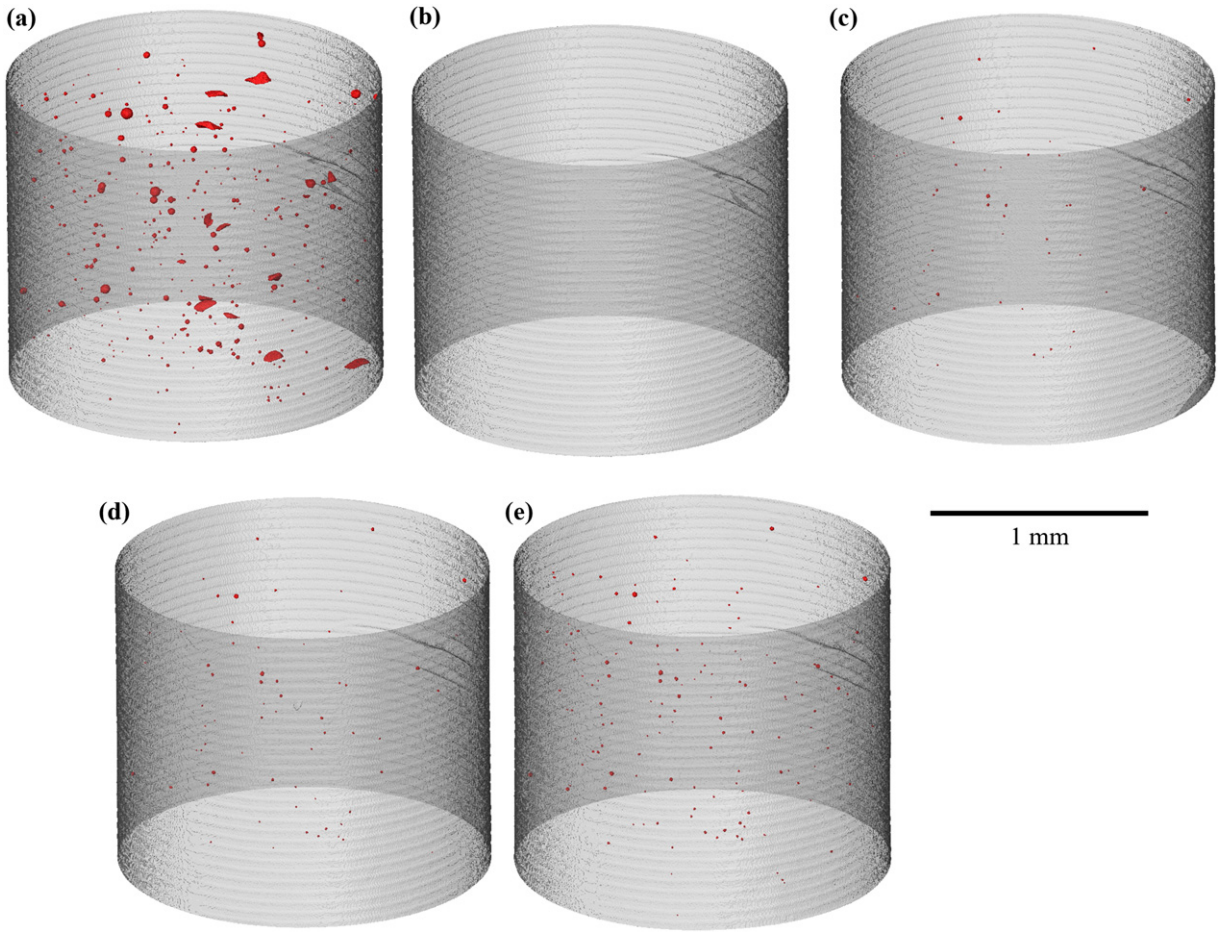

Fig. 1. 3D visualisation of the porosity (red) imaged by CT scans of the same cylindrical sample (build direction vertical) (a) as-built; (b) following HIPing; (c) 10 min at 1035 °C; (d) 10 h at 1035 °C; and (e) 10 min at 1200 °C.

X-ray CT scanning was undertaken using a Xradia Versa 500 machine on the mid-section of the (~1.5 mm height) cylindrical sample, using the procedure fully described in ref. [5]. Under these conditions, a 2 μm voxel size was achieved allowing the reliable identification of defects with an equivalent (sphere of equal volume) diameter greater than 5.2 μm. The CT data was analysed using Avizo 9.0 software.

Three heat treatments were applied sequentially to the HIPed sample in the following order: HT1, 10 min at 1035 °C (1308 K); HT2, 10 h at 1035 °C; and HT3, 10 min at 1200 °C (1473 K). The first heat treatment (HT1) was chosen to replicate a typical β-anneal employed by the aerospace industry, while HT2 and HT3 were used to study the effect of increasing the hold time and maximum temperature, respectively. To avoid oxidation, all heat treatments were performed in a vacuum furnace at <1 Pa, using a heating ramp rate of 5 K/min and allowed to cool to ambient temperature under vacuum. After each heat treatment, the same mid-section of the cylindrical sample was rescanned by CT and the data spatially realigned, to correlate between scans the behaviour of any pores that were present.

Fig. 1 shows a 3D visualisation of the pores detected in the cylindrical sample as-machined from the built cuboid, and following HIPing and the three sequential heat treatments described above. It should be noted that in the as-built condition, at this location near the edge of the sample, the volume fraction of LOFDs was high in comparison to that seen in the centre of an as-manufactured build, where LOFDs typically make up only a minor fraction of the pore population [3,5]. The contour strategy, used to melt the edge of SEBM samples, has been shown to contain a greater number density of LOFDs, in comparison to the hatching strategy used to melt the internal area [5].

From Fig. 1b it is apparent that after HIPing no pores can be detected in the scanned volume shown, and this is confirmed by the statistical data presented in Table 1. However, following the first heat treatment step (HT1), CT analysis revealed the presence of some small pores. Following the second and third heat-treatment, more and larger pores became evident. It is notable from Table 1 that increasing the hold time (HT2) led to less pore growth than increasing the hold temperature (HT3).

From visual inspection of the 3D projections given in Fig. 1 it is hard to correlate the as-manufactured pores through the HIPing and heat treatment stages. However, in Fig. 2 the evolution of a single pore is shown. Detailed analysis has confirmed that all the pores appearing during the heat treatment stages can be correlated to the locations of pores in the original build. Evidently such pores (Fig. 2a) had shrunk/disappeared during HIPing (Fig. 2b), before reappearing and growing during the subsequent heat treatment steps (Fig. 2c–e).

Table 1
Statistical data from quantification of all the pores detected in the same sample, as-built, and following HIPing and annealing.

Condition	Volume fraction (%)	Number	Mean equiv. dia. (μm)	Max. equiv. dia. (μm)
As-built	0.0397	309	13.3	53.3
HIPed	0.0000	0	–	–
HT1	0.0007	49	8.4	18.6
HT2	0.0011	63	9.2	20.0
HT3	0.0026	140	9.4	21.6

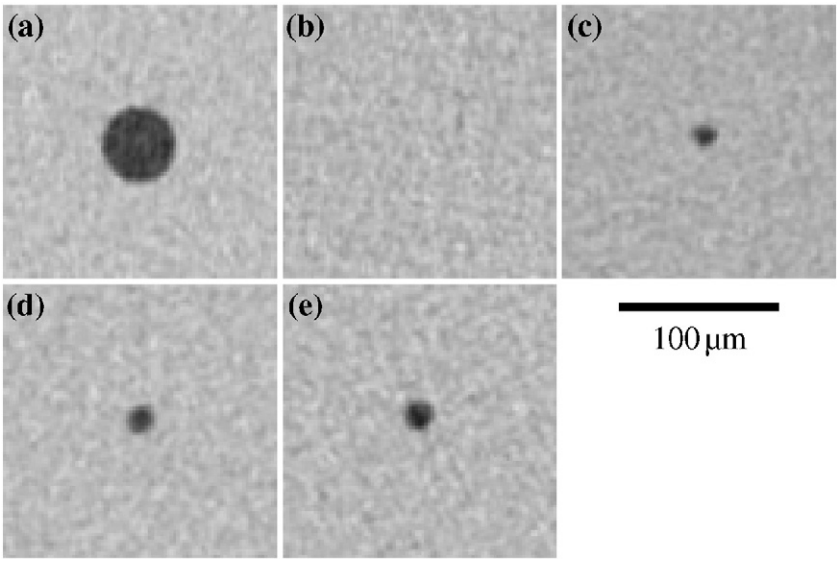

Fig. 2. Example slice of the CT data centred on an individual pore (a) as built, (b) same location after HIPing, (c) HT1, (d) HT2 and (e) HT3.

In Fig. 3 pore sizes have been plotted against their aspect ratio for all the pores detected within the as-built sample. The subsequent CT datasets were correlated against these to identify those pores that reappeared upon heat treatment. From this analysis, it is immediately apparent that the large, high aspect ratio LOFDs present in the build were successfully removed by HIPing and did not reappear on heat treatment. By contrast, all of the larger (>20 μm diameter for HT1, >18 μm for HT2 and >12 μm for HT3), nearly spherical pores, whose morphology is consistent with them being gas pores, could be resolved upon heat treatment in the CT scans (i.e. they regrew to have an equivalent diameter >5.2 μm).

In Fig. 4 the as-built pore sizes of all the pores that reappeared on annealing have been plotted against their corresponding sizes measured after each heat treatment step. The data shows a clear positive correlation, indicating that after heat treatment the pores have regrown in proportion to their original size, but always remained smaller than in the as-built sample, even after a more extensive heat treatment. In addition, it is notable that the higher temperature treatment is more effective at increasing the pore size than increasing the hold time.

While the great majority of the pores appear to grow according to a similar trend, an individual pore is highlighted (ellipse) that appears to depart from this behaviour, apparently growing at a much slower rate.

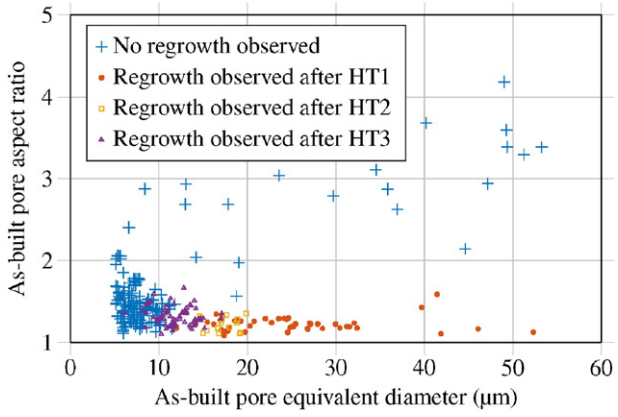

Fig. 3. Quantification of all the pores as-manufactured, with those that were found to reappear after annealing indicated.

Closer inspection of the CT data for this pore (inset in Fig. 4) shows that in the as-built condition it comprises two gas pores in very close proximity, possibly in the process of coalescing. Due to the resolution limit and segmentation technique used, these two pores were quantified as a single larger void in the as-built sample, whereas following HIPing and heat treatment the pores had regrown as two distinct, much smaller voids.

The results presented here demonstrate that, even after annealing, HIPing should reduce the detrimental effect of the pores on the fatigue life, as, even though some of the pores regrow, they are fewer and smaller than the defects found in an as-built part. Importantly, HIPing is effective in removing the more dangerous, high aspect-ratio, LOFDs, which do not seem to regrow during annealing. Only those pores identified as gas pores appear to regrow upon annealing, and regrow in proportional to their initial volume (Fig. 4). Their reappearance during annealing can be explained by considering that the origin of such gas pores lies in argon trapped in the powder particles melted in the SEBM process. Argon is unable to diffuse out of the material during HIPing [7] and thus remains in the sample within small collapsed pores, but with a higher internal pressure [6]. Upon heat treatment, this high internal gas pressure will provide a driving force for pore regrowth.

Metallographic examination of similar HIPed SEBM samples by Gaytan et al. [9] has previously revealed the presence of some remnant pores, that had greatly reduced in size and collapsed to leave a contacting interface area that has not fully bonded. Such a small size and thin pore morphology would be extremely difficult to detect by CT. However, it is apparent that if such small pores contain a high enough gas pressure after HIPing, on the application of a high temperature heat treatment, they can regrow sufficiently to become re-detectable. The regrowth of argon porosity is known to occur in HIPed titanium powder compacts containing small argon pores when they are heat treated close to, or above, the β-transus [10]. In fact, the expansion of high pressure argon filled pores generated by HIPing powders has been deliberately exploited to produce titanium foams [11,12]. In contrast, and despite the prevalence of argon atomised titanium powders being used as feedstock materials [1,2,5,9], to date, apart from the work presented here, there has been no other report of pore regrowth being observed in HIPed AM components.

The failure of LOFDs to regrow can be explained by considering that they originate from insufficient overlap of the melt tracks. In the SEBM process, which is performed under vacuum, they therefore do not contain a residual gas pressure after HIPing sufficient to drive their regrowth. However, in processes carried out under an argon atmosphere, such as

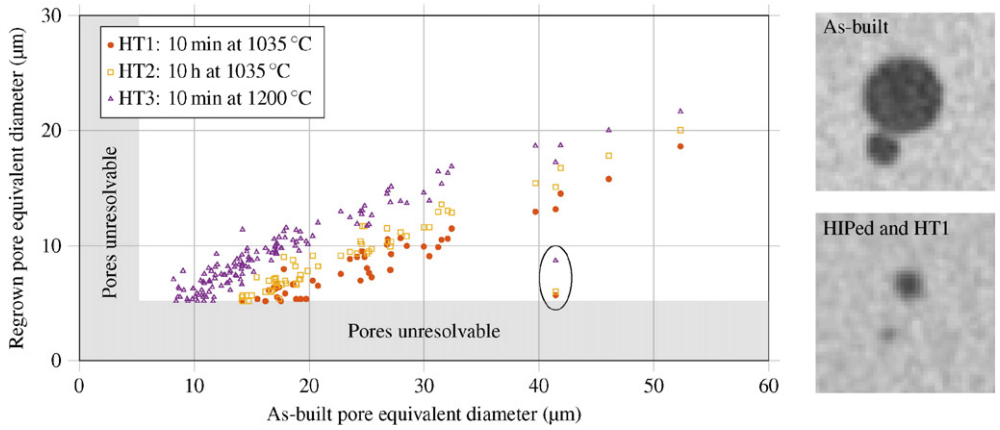

Fig. 4. The size of those pores that reappeared after each annealing step correlated to their as-built size. The inset shows a pair of pores which were identified as a single pore in the analysis (marked by the ellipse in the plot).

selective laser melting, LOFDs could contain sufficient argon to survive and regrow from the small size they shrink to after HIPing, due to the gas pressure, although they would be expected to reform with a more spherical morphology, which would reduce the stress concentration they generate.

The physics governing the expansion of the pores is complex and will not be considered in detail here. However, it is clear from the experimental data that, in this case, the expansion was influenced by, among other factors, the annealing temperature, hold time and initial pore volume. Pore growth will be opposed by the energy required to increase the surface area of the pores and deform the surrounding material. Previously, the time dependent growth of argon filled gas pores has been attributed to creep deformation of the surrounding material [11,12]. In a standard creep test, where samples are tested at a constant stress, a high initial transient strain rate is often observed before the strain rate slows and remains approximately constant until necking [13]. Our observation that increasing the hold time by a factor of 60 (from 10 min (HT1) to 10 h (HT2)) results in only a ~3 μm increase in pore diameter (Fig. 4) also reveals that the most rapid expansion of the pores, and thus highest strain rate, occurs early in the heat treatment.

In contrast to a standard creep test, the pressure exerted on the material will not have been constant throughout the annealing steps. The lack of any significant diffusion of argon in titanium means the number of moles of argon per individual pore can be assumed to remain constant once initial solidification has taken place. Thus, from the ideal gas law, the pressure within each pore can be estimated as:

$$P_2 = P_1 \cdot (V_1/V_2) \cdot (T_2/T_1) \quad (1)$$

where: P, V and T are the pressure (Pa), volume (m^3) and temperature (K) respectively; and the subscripts 1 and 2 indicate values from two conditions, for example during HIPing and a heat treatment. It is clear from Eq. (1) that during an isothermal heat treatment the pressure exerted by the argon gas will decrease as the pore enlarges, reducing the driving force for growth and leading to a reduction of the expansion rate. Hence, at a given temperature it is likely that individual pore sizes will follow an approximately logarithmic trend with time, and will reach a size where the pressure diminishes to a level where the rate of further pore growth becomes negligible. Indeed, this is what has been observed in other studies when deliberately re-growing a much larger initial volume fraction of HIPed argon pores to a much greater final volume fraction [11,12] and also aligns well with our limited data regarding the effect of time (HT1 and HT2).

When the hold temperature was increased to 1200 °C for ten minutes (HT3), after applying the prolonged 10-hour treatment at 1035 °C, the increase in pore volume fraction detected became dramatically larger because, in addition to slightly raising the pore pressure, a higher temperature increases the creep rate for a given applied stress. It is thus apparent that the β-annealing temperature after HIPing is of greater importance in determining pore regrowth than heat treatment time.

To summarise, it has been conclusively demonstrated that the application of high temperature β-annealing treatments can cause porosity to reappear in HIPed SEBM Ti–6Al–4V components, even after relatively short treatment times (10 min at 1035 °C). Using non-destructive X-ray CT, the pores have been tracked, confirming that those that reappear have a position and size that can be correlated to gas pores present in the original build. These shrink below the detection limit of CT during HIPing. Pore expansion is caused by the high pressure within the pores which remain after HIPing due to the low diffusivity of argon in titanium. Rapid growth of the pores occurs early in the heat treatment, before slowing due to the decrease in argon pressure as the pores expand. Increasing the hold temperature leads to greater growth of the pores due to a small increase in argon pressure and reduced resistance to deformation.

Acknowledgments

Thanks to Julia Behnsen and Fergus McCool for providing assistance with setting up the CT and furnace equipment respectively. The authors acknowledge EPSRC funding from the designing alloys for resource efficiency (DARE) program (EP/L025213/1), the Centre for Doctoral Training in Advanced Metallic Systems (EP/L016273/1), and the Henry Moseley X-ray Imaging Facility (EP/F007906/1, EP/F001452/1 and EP/M010619/1). For access to the original data used please contact the corresponding author.

References

[1] I. Gibson, D.W. Rosen, B. Stucker, Additive Manufacturing Technologies, first ed. Springer, London, 2010.
[2] W.E. Frazier, J. Mater. Eng. Perform. 23 (2014) 1917–1928, http://dx.doi.org/10.1007/s11665-014-0958-z.
[3] H. Gong, K. Rafi, H. Gu, T. Starr, B. Stucker, Addit. Manuf. 1 (2014) 87–98, http://dx.doi.org/10.1016/j.addma.2014.08.002.
[4] A.A. Antonysamy, Microstructure, Texture and Mechanical Property Evolution during Additive Manufacture of Ti6Al4V alloy using Laser, Electron Beam, and Arc Melting Techniques for Aerospace ApplicationsPhD Thesis University of Manchester, 2012 (https://www.escholar.manchester.ac.uk/uk-ac-man-scw:160535).
[5] S. Tammas-Williams, H. Zhao, F. Léonard, F. Derguti, I. Todd, P.B. Prangnell, Mater. Charact. 102 (2015) 47–61, http://dx.doi.org/10.1016/j.matchar.2015.02.008.
[6] S. Tammas-Williams, P.J. Withers, I. Todd, P.B. Prangnell, Metall. Mater. Trans. A 47 (2016) 1939–1946, http://dx.doi.org/10.1007/s11661-016-3429-3.
[7] H. Atkinson, S. Davies, Metall. Mater. Trans. A 31A (2000) 2981–3000, http://dx.doi.org/10.1007/s11661-000-0078-2.

[8] C.J. Smith, F. Derguti, E.H. Nava, M. Thomas, S. Tammas-Williams, S. Gulizia, D. Fraser, I. Todd, J. Mater, Process. Technol. (2015), http://dx.doi.org/10.1016/j.jmatprotec.2015.08.028.
[9] S.M. Gaytan, L.E. Murr, F. Medina, E. Martinez, M.I. Lopez, R.B. Wicker, Mater. Technol. Adv. Perform. Mater. 24 (2009) 180–190, http://dx.doi.org/10.1179/106678509X12475882446133.
[10] F.H. Froes, D. Eylon, Int. Mater. Rev. 35 (1990) 162–184, http://dx.doi.org/10.4028/www.scientific.net/KEM.77-78.115.
[11] N.G.D. Murray, D.C. Dunand, Acta Mater. 52 (2004) 2269–2278, http://dx.doi.org/10.1016/j.actamat.2004.01.039.
[12] N.G.D. Murray, D.C. Dunand, Acta Mater. 52 (2004) 2279–2291, http://dx.doi.org/10.1016/j.actamat.2004.01.019.
[13] H.J. Frost, M.F. Ashby, Deformation-mechanism maps: the plasticity and creep of metals and ceramics, first ed. Pergamon Press, Oxford, 1982.